19th Brazilian Congress of Thermal Sciences and Engineering
November 06th-10th, 2022, Bento Gonçalves - RS - Brazil

ENC-2022-0299
EXPERIMENTAL STUDY OF FLUID-STRUCTURE INTERACTION OF A MODEL OF DOWN-HOLE SAFETY VALVE SUBJECTED TO SLUG FLOW

Luis F. Acuña-Alegría
University of São Paulo (USP), São Carlos School of Engineering (EESC), Mechanical Engineering Department, Industrial Multiphase Flow Laboratory (LEMI), Av. Trab. São Carlense, 400 - Parque Arnold Schimidt, São Carlos - SP, 13566-590, Brazil.
facuna.alegria@usp.br
Marlon M. Hernández-Cely
Engineering Center, Federal University of Pelotas, Rua Benjamin Constant, n° 989, Porto, Pelotas 96010-020, RS, Brazil.
marlonhc@usp.br

Oscar M. H. Rodriguez
University of São Paulo (USP), São Carlos School of Engineering (EESC), Mechanical Engineering Department, Industrial Multiphase Flow Laboratory (LEMI), Av. Trab. São Carlense, 400 - Parque Arnold Schimidt, São Carlos - SP, 13566-590, Brazil.
oscarmhr@sc.usp.br

Abstract. *The governing differential equation that describes the two-phase-fluid/structure interaction is used in its dimensionless form to scale up geometric terms of a problem associated with a typical down-hole safety valve (DHSV) used in oil wells. The DHSV has as main function the prevention of spills of hydrocarbons in offshore production. The motivation is an actual report of DHSV failures, which may be linked to vibrations of high amplitude and low frequency induced by internal two-phase flow, probably in the slug flow pattern. Scaling up was done with special attention, not only due to the usual geometric, kinematic and dynamic conditions that must be fulfilled to assure similarity, but also because of some two-phase flow characteristics that add complexity to the analysis. Real field information from the oil and gas industry was used to obtain the geometry of the valve's model and the dynamically similar flow conditions. The scaling-up is done in a simplified way considering a valve working fully open, i.e., the valve behaves as a part of the tube, but with a constriction at its inlet. Experimental tests are carried out with air and water at 200 (kPa abs.) and room temperature at several volumetric flows, strategically chosen according to the information available in the two-phase flow map constructed for this particular purpose.*

Keywords: *Fluid-structure Interaction (FSI), Flow-induced Vibrations (FIV), Two-phase Flow, Down-Hole Safety Valve (DHSV), Scale-up.*

1. INTRODUCTION

1.1 Literature Review

Due to the dynamics surrounding the physical configuration adopted by the fluids during the flow, the need arises to open the field of knowledge for studies focused on the two-phase-flow/structure interaction. In this context, several authors have proposed methodologies for coupling the Navier-Stokes equations with the structural dynamics equations (Ni et al., 2019) to obtain a relationship between structural loads and fluid flow, since according to Ribeiro and Pedroso (2016, the effects produced by fluids are capable of influencing the magnitude, frequency and stability of the system. Furthermore, to date, problems related to this matter have not yet been able to be modeled with sufficient precision, let alone analytically (Tian et al., 2020).

Currently, the literature offers several works oriented to the study of two-phase-flow/structure interaction, but few aimed at the study of Two-Phase Flow Induced Vibrations (2-FIV). A work that can be cited is the research by Li et al. (2020), who used the mathematical expression proposed by Païdoussis (2014) and through a numerical method called Generalized Integral Transform Technique (GITT) the structural behavior of the vertical tube when exposed to a two-phase flow was modeled, with the objective of determine the effect of damping and thereby avoid excess flow-induced vibrations.

Cabrera-Miranda and Paik (2019) mention that when a two-phase flow adopts a slug-type pattern, it generates structural vibrations that lead to fatigue failures precisely because of the intermittent characteristics of this pattern is

composed of large gas bubbles that flow alternately with liquid pistons with random frequencies (Miwa et al., 2015; Ortega et al., 2018), generating pressure, density and velocity fluctuations that contribute in the structural response (Zhu et al., 2019). In addition, effects such as compressibility and gas expansion make the variation in momentum between both fluids not negligible and have a significant influence on the dynamic behavior of the tubes (Wang et al., 2018). For these reasons, the intermittent pattern is considered more aggressive than the others (Miwa et al., 2015).

Based on the information given above, the following subsection will analyze real data belonging to a company in the sector, to justify the research theme of this work. Next, details associated with the experiments will be delivered, which will be carried out at the Laboratory of Industrial Multiphase Flows (LEMI) of the University of São Paulo (USP): geometric design of a valve model and the two-phase flow conditions that will serve to measure the vibrational responses of said valve. Finally, some results that intend to be collected will be presented, based on the work od other researchers since the results themselves are still under development.

1.2 Research Justification

Ensuring safety during the oil and gas extraction process is essential to avoid accidents, both leaks into the sea and human deaths. In this sense, safety valves are responsible for acting when irregularities are detected during operation. However, companies in the Brazilian oil sector are concerned that the life of those devices is shorter than that reported by supplied. This is because regulations, such as API 14A (2015), only consider laboratory tests with single-phase flows such as water and nitrogen, forgetting the possible presence of a two-phase flow inside the valve when it is already installed in the field.

A simplified analysis to determine if there is a relationship between the type of flow and safety valve failures is done. For this, taking advantage of the fact that a company in the sector provided information regarding 160 wells, the theory of the homogeneous model was used to determine whether in the area where the safety valve is installed, the consideration of two-phase flow is applied. In this context, since the theory used for this analysis is simplified, the following criterion is adopted:

- If the volumetric fraction is less than 0.4 the flow is treated as single-phase;
- If the volumetric fraction is greater than 0.4 the flow is treated as two-phase.

The criterion defined above is due to the fact that when the slip between both phases is considered, the void fraction decreases since, in addition to depending on the volumetric fraction, it also depends on other parameters such as the distribution parameter and the weighted mean drift velocity. Consequently, necessarily the void fraction decreases enough so that the flow can be treated as single-phase or not. However, it is important to note that the information obtained from the analysis is preliminary and only serves as a starting point to justify the research theme of this work.

Thus, two graphs are presented in sequence, showing the results obtained in the analysis. Note that, of the 160 wells studied, 66% (105 units) would have a two-phase flow in the zone of interest (see Figure 1.1a). Likewise, analyzing only the wells where the safety valve failed (see Figure 1.1b), 89% (33 of the 37 units) would correspond to a valve that failed and at the same time showed a two-phase flow.

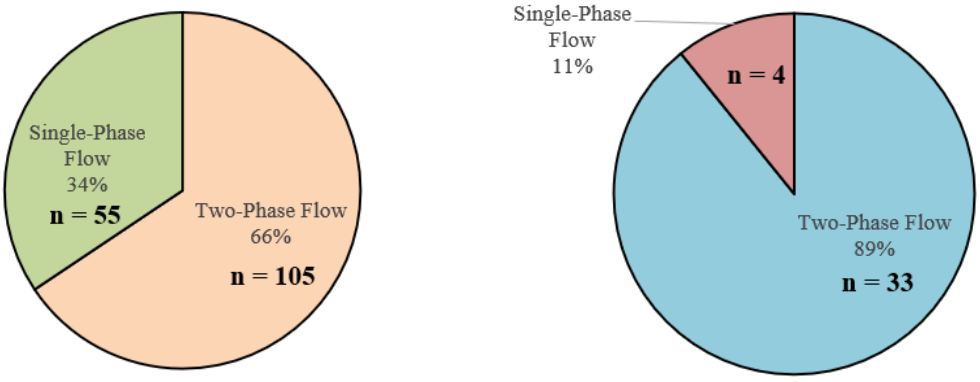

a) b)

Figure 1.1. Real well data analysis: a) according to flow type, b) valve failures associated with flow.
Source: Own.

Based on this information, the presence of two-phase flow in the hydrocarbon extraction line seems to be evident. Likewise, there seems to be a connecting between the type of flow and the failures that the safety valve may present. This connection may be related to flow-induced vibrations (FIV), which if prolonged over time, will produce wear on elements that will consequently fail. Due to this, a two-phase-flow/structure study should be developed with the

objective of estimating the life of a device under a certain operating condition and, in this way, scheduling maintenance times.

2. METHODOLOGY

2.1 Experimental Apparatus

The experimental tests will be carried out on a reclining table (see Figure 2.1) which has a high- and low-pressure circuit through which 4 different fluids flow: Lubrax Turbina 22, dense gas (*Hexafluoreto de Enxofre*), water and air. The experimental bench is located in the Industrial Multiphase Flow Laboratory (LEMI) belonging to the São Carlos School of Engineering (EESC) of the University of São Paulo (USP).

Figure 2.1. Reclining table.

In this work, for the development of the experiments, only two fluids will be used: water and air, which will flow in the line of 2 (in) at a pressure of 100 (kPa man.).

The tests will be carried out in the vertical direction because the research interest is focused on the vibrational determination of a simplified model of a safety valve, the one that is typically installed in pre-salt oil and gas production lines.

The diagram presented below (see Figure 2.2) shows in detail the experimental apparatus with the components and instruments needed to carry out the research. In the figure, it is visualized how the Pump (B) pushes water from the tank at a certain pressure, which is dominated by the rotation velocity of that pump through the Frequency Inverter (IF). On the other line, there is the compressor (C) that pushes air to the accumulator tank and, in this way, is released according to the demand through a valve. Both the water line and que airline contain sensors that allow keeping control of some properties of interest such as volumetric flow (FL), temperature (TT) and pressure (TP). Note that the airline has a control valve (VC) that allows you to regulate the volumetric air flow using LabVIEW software. Then, at the mixing point (Y), the water and air flow through a single line and after a certain length, the water-air mixture enters the model valve (DHSV) and the vibrations produced by the flow are measured with uniaxial piezoelectric accelerometers (CCLD/IEPE) (A). Also note that, at the output of the model valve, there are also pressure (TP) and temperature (TT) sensors to keep control of these properties in this zone. Finally, note that at the ens of the model valve there are two quick-closing valves (VFR), which serve to experimentally measure the volumetric fraction of the two-phase flow.

The nomenclature of the elements is indicated in the sequence (see Tables 2.1 and 2.2).

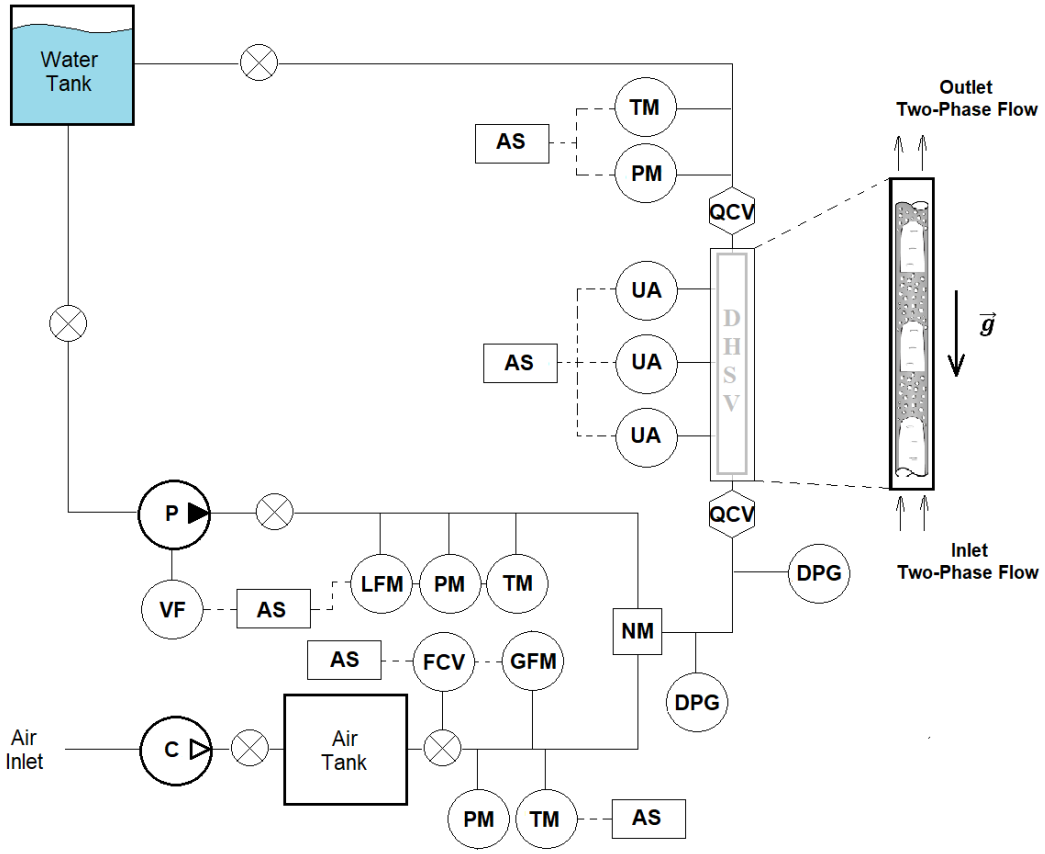

Figure 2.2. Experimental apparatus.
Source: Own.

Table 2.1. Experimental apparatus components.

Nomenclature	Component
P	Pump
C	Compressor
FV	Frequency Variator
FCV	Flow Control Valve
QCV	Quick Closing Valve
NM	Nozzle of Mixture
AS	Acquisition System

Table 2.2. Description of the instruments that make up the experimental bench.

Nomenclature	Component	Measuring Range	Precision
LFM	Liquid Flow Meter	0,50 – 79 (m^3/h)	± 1%
PM	Pressure Meter	0 – 1200 (kPa)	± 0,25%
TM	Temperature Meter	0 – 100 (°C)	± 0,15 + 0,02 $\|T\|$
GFM	Gas Flow Meter	1,37 – 100 (m^3/h)	± 1%
DPG	Differential Pressure Gauge	0 – 10 (kPa)	-
UA	Uniaxial Accelerometers	0,2 – 12800 (Hz)	± 2%

2.2 Experimental Conditions

Due to the large dimensions of the prototype, it is impossible to carry out experiments with a real valve, therefore, experiments with a model valve must necessarily be considered. In this sense, consider the fourth-order linear differential equation (PDE) employed by Li et al. (2020), between others, which represents the two-phase-flow/structure interaction phenomenon in this work:

$$EI\frac{\partial^4 y}{\partial x^4}+\left(\sum_k M_k+m\right)g\left((x-L)\frac{\partial^2 y}{\partial x^2}+\frac{\partial y}{\partial x}\right)+\sum_k M_k U_k^2\frac{\partial^2 y}{\partial x^2}+2\sum_k M_k U_k\frac{\partial^2 y}{\partial t\,\partial x}+\left(\sum_k M_k+m\right)\frac{\partial^2 y}{\partial t^2}$$
$$+EI\frac{\mu}{\Omega}\frac{\partial}{\partial t}\left(\frac{\partial^4 y}{\partial x^4}\right)+k\frac{\partial y}{\partial t}=0 \quad (1)$$

Where EI is the flexural rigidity; $y(x, t)$ is the transversal displacement; M_k and U_k are respectively the mass per unit length and steady flow velocity of the gas and the liquid phases where the subscript k indicates the phase (k = 1 if the fluid is gas and k = 2 if the fluid is liquid); m is the mass of the pipe per unit length; g is the gravitational acceleration; σ is the structural damping coefficient; Ω is the circular frequency; and, C is the damping coefficient of fluids.

Note that the last two terms on the left-hand side, represent the damping of the system. Specifically, the term $EI\frac{\sigma}{\Omega}\frac{\partial}{\partial t}\left(\frac{\partial^4 y}{\partial x^4}\right)$ is the structural damping and the term $C\frac{\partial y}{\partial t}$ characterize the fluids damping (two-phase flow).

To relate each of the different effects between the prototype and the model, it is necessary to dimensionless the equation presented above in order to obtain dimensionless parameters that are able to adequately represent the physical phenomena. In this context, the dimensionless parameters for this problem are:

$$\xi=\frac{x}{L};\ \eta=\frac{y}{L};\ \tau=\left(\frac{EI}{\sum_k M_k+m}\right)^{1/2}\frac{t}{L^2};\ \omega=\frac{\mu}{\Omega L^2}\left(\frac{EI}{\sum_k M_k+m}\right)^{1/2};\ u_k=\left(\frac{M_k}{EI}\right)^{1/2}U_k L;\ \beta_k=\frac{M_k}{\sum_k M_k+m};$$
$$\gamma=\left(\frac{\sum_k M_k+m}{EI}\right)gL^3;\ \kappa=kL^2\left(\frac{1}{(\sum_k M_k+m)\,EI}\right)^{1/2} \quad (2)$$

The similarity theory ensures that ideally all dimensionless parameters should be guaranteed between the prototype and the model, however this cannot always be covered (Çengel and Cimbala, 2006). Therefore, it is preferable to have a low number of dimensionless parameters (if possible) because in this way the convergence of similarity results between the parameters can be guaranteed (Shoham, 2005).

3. RESULTS AND DISCUSSION

3.1 Prototype Data Processing

Of the 160 well data analyzed in the introductory part of this document to determine whether it is possible to apply the two-phase flow theory, only 138 data from the total wells are processed to build the flow maps and determine, from the total wells, those that present an intermittent flow pattern (slug or churn flow). The reason why 138 wells were chosen from a total of 160, is because among these data 2 different diameters were found, thus allowing a more uniform analysis in the data processing. In this context, using the model by Taitel et al. (1980) for the real data of 5.5 (in) e 6.625 (in) diameters wells, respectively, we obtain:

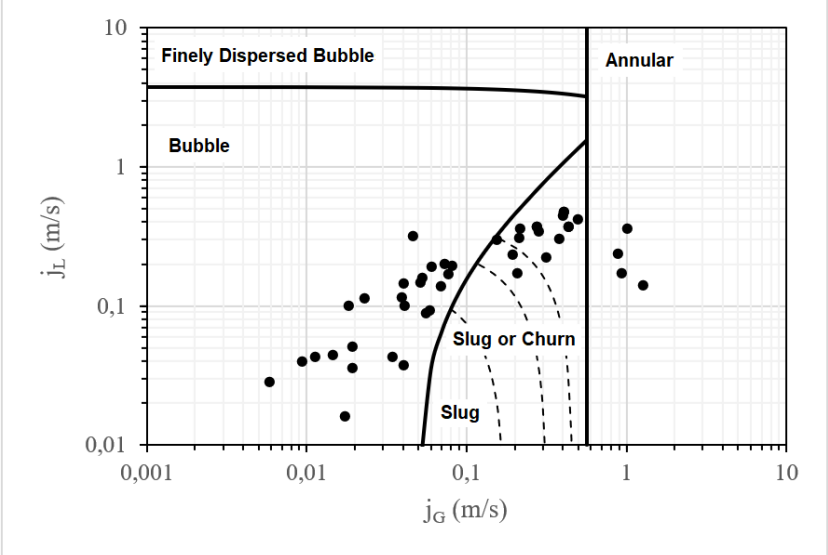

a)

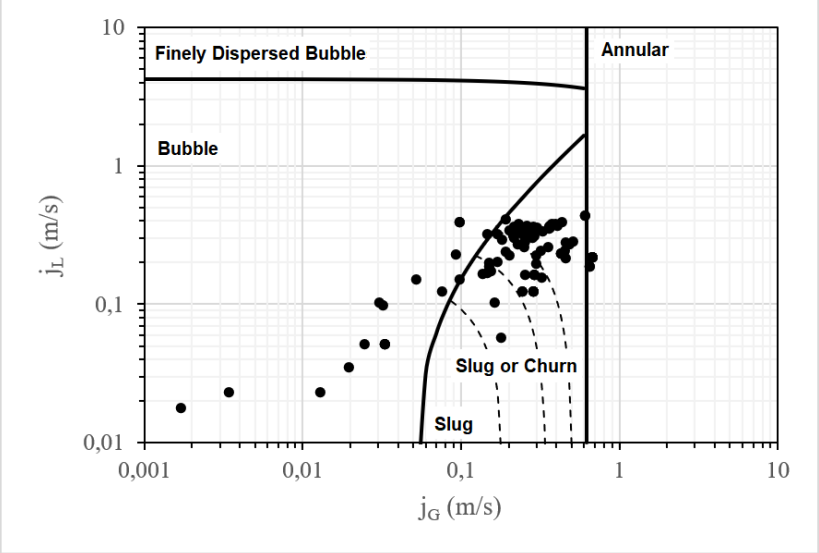

b)

Figure 2.3. Flow map for a diameter valve: a) 5.5 (in) (44 data); b) 6.625 (in) (94 data).
Source: Own.

Note that of the 138 wells included in the flow maps (see Figure 2.3), 85 are within the desired limits (intermittent pattern), therefore, only the information associated with these wells is considered to scale between the actual situation (prototype) and experimental situation (model).

In this way, using simplified information associated with the geometry of the real valve (prototype) (see Table 2.3), the dimensionless parameter γ (see Eq. 2) can be determined.

Table 2.3. Prototype geometric relationship.

Length	Outside diameter	Inner diameter
34.6020	1.8754	1.0000

The choice of that parameter to dimension the model valve is based on the justification that the γ encompasses several effects indicated below:

- Hydrodynamic parameters: $\Sigma\,(M_k + m)$;
- Structural parameters: EI;
- Forces associated with gravity: g;
- Element length: L^3.

Therefore, the parameter γ is used as a starting point to determine the length of the model valve. In this sense, using the information associated with the 85 wells that showed intermittent two-phase flow in the real valve area, one arrives at that parameter γ is:

Diameter (in)	N° wells	γ (-)	$\gamma_{médio}$ (-)
5.5	16	0.008154867	0.009494769
6.625	69	0.009805471	

So, imposing internal and external diameters for the model valve equal to: 0.0519 (m) e 0.0603 (m), respectively, the length L will be: 2.13 (m). Note that the value of L is obtained by considering tests in the laboratory with water and air, under a gauge pressure of 100 (kPa) and a temperature of 27°C (approximately ambient temperature).

For the calculations, volumetric fractions between 0.5 e 0.95 (predicted using the homogeneous model) were considered, because when including the slip between the phases, the magnitude of these volumetric fractions will be corrected. The important thing is that the experimental conditions defined for the laboratory tests are within the limits that demarcate the intermittent pattern in the flow map.

Once the model valve geometry is defined, the flow conditions can be determined using another dimensionless parameter: u_k. In this case, the only unknown is the velocity U_k, since the remaining parameters are known. Because the theory of the Homogeneous Model is being used, the term U_k becomes j, that is, the volumetric flux. Thus, in the flow

map, the flow conditions that meet the condition were identified: $u_{k_{protótipo}} = u_{k_{modelo}}$, corresponding (from left to right) to volumetric fractions of 0.5; 0.6; 0.7; 0.8; 0.9 and 0.95. Furthermore, all the experimental conditions defined in the flow map are within the margins demarcated by the intermittent flow pattern, are discussed above. Consequently, $u_{k_{protótipo}}$ is:

Diameter (in)	N° wells	u_k (-)	$u_{k_{médio}}$ (-)
5.5	16	0.001564327	0.00131338
6.625	69	0.001255192	

3.2 Model Valve and Intermittent Pattern Flow

In the model valve, only an internal restriction will be included right after the fluids inlet (see Figure 2.4), so that there is an acceleration during the flow that generates vibrations as a result of the turbulence provided by the length of mixture formed at that point. In the design of the real valve, this contraction is before the flapper, however, in the model valve this is not being considered because during the normal operation of the real valve it is open, behaving as if it were part of the pipeline. Remember that the flapper only operates when high pressures or flows are detected, therefore, these are particular situations that do not represent the usual behavior of the hydrocarbon extraction operation. In this context, as the study of this research is to evaluate the vibrations induced by flow, the model valve does not need to have a flapper.

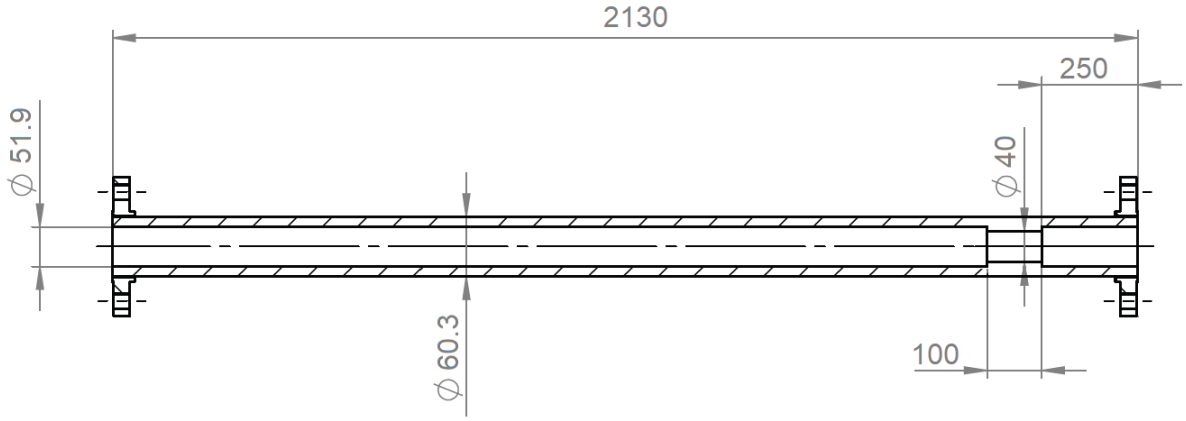

Figure 2.4. Model valve (dimensions in millimeters).
Source: Own.

To define the flow conditions for the experiment in the laboratory, water and air will be used with a pressure of 200 (kPa abs.) and a temperature of 27°C (approximately ambient temperature). Associated properties such as density and viscosity are indicated in the table below.

Table 2.4. Fluid properties employed in the experiment.

P (kPa)[(1)]	T (°C)	AIR		WATER	
		ρ_G (kg/m^3)	μ_G (Pa s)	ρ_L (kg/m^3)	μ_L (Pa s)
200	27	2.32	1.856 x10^{-5}	996.6	8.514 x10^{-4}

(1) the pressures indicated in the table are absolute.

Using the mathematical expressions associated with the model by Taitel et al. (1980), it is possible to construct flow maps for the fluids: water-air (see Figure 2.5), according to the conditions listed in Table 2.4. With this, together with the imposed condition of the dimensionless parameter $u_{k_{protótipo}} = u_{k_{modelo}}$, the operating conditions suitable for reproducing in the laboratory are discovered.

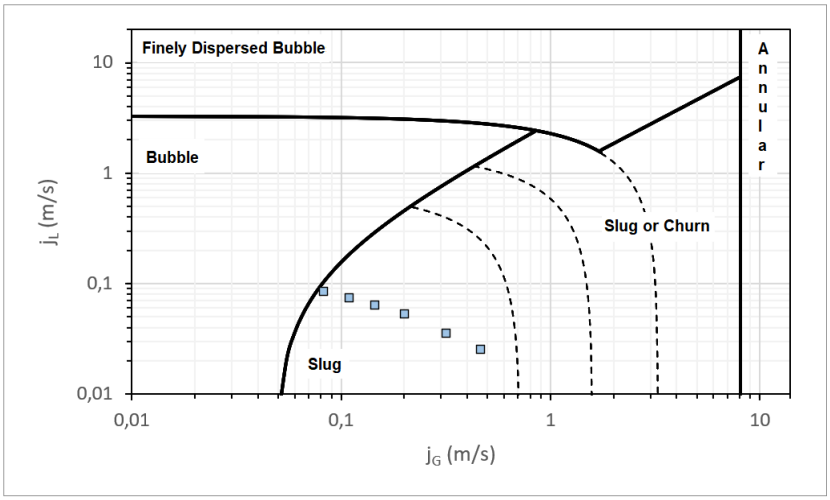

Figure 2.5. Experimental matrix plotted in the flow map.
Source: Own.

The discrete points indicated on the flow map are, in short, the experimental matrix. However, it will not be possible to reproduce these conditions in the laboratory, since the volumetric flows associated with these superficial velocities are very low and the available meters will not be able to detect the presence of fluids. Though, applying the basic foundation of the theory associated with accelerated tests, the following experimental tests are proposed for this work (see Figure 2.6):

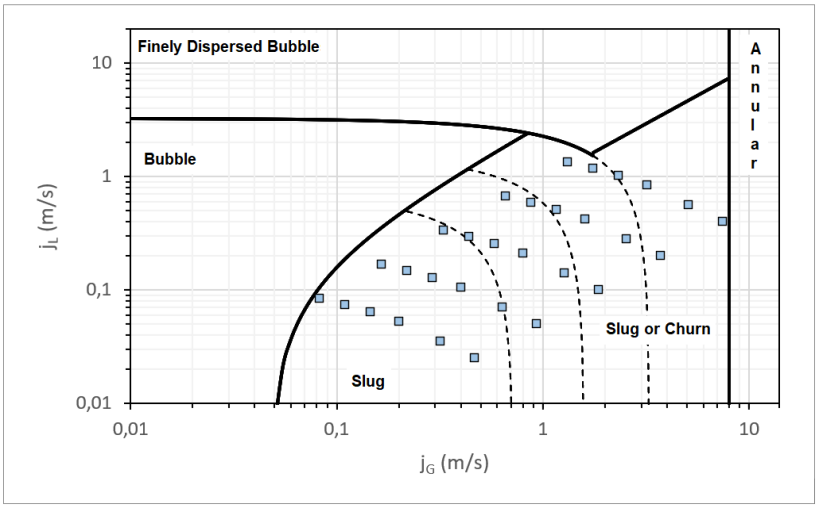

Figure 2.6. Experimental matrix plotted in the flow map according with acceleration tests.
Source: Own.

The choice of new experiments was made considering increments of surface velocities in 2, 4, 8 and 16 times with respect to the surface velocities originally obtained. In this way, the dimensionless velocity $u_{k_{modelo}}$ will also change in the same proportion. Finally, once the experiments are done and the results are processed, it will be possible to extrapolate corresponding to the original condition and, consequently, analyze the behavior of the prototype for a given condition.

3.3 Expected Results

Among the preliminary results, it is expected to obtain behaviors such as that obtained by Carvalho et al. (2020), where larger vibration amplitudes appear in the transition region between the Taylor bubbles and the liquid piston (see Figure 3.1a). Similar results were reported by Matos et al. (2022), where the intermittence of the phases produces different amplitudes in the time domain (see Figure 3.1b).

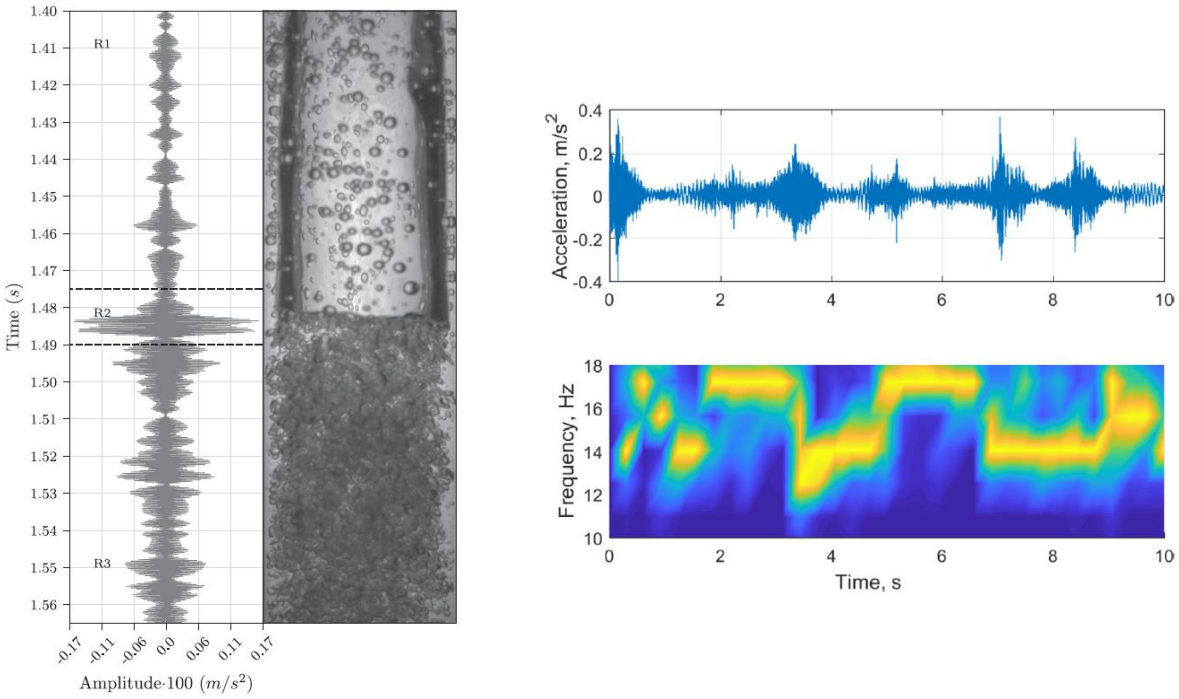

a) b)

Figure 3.1. Vibrational results obtained in some associated works: a) Carvalho et al. (2020); b) Matos et al. (2022).

Additionally, it is interesting to comment from Figure 3.1b that, in the Time vs Frequency graph, a cyclic behavior for two fundamental frequencies at 14 (Hz) and 17 (Hz) is presented, which is equivalent for a specific operating condition. In this sense, if the flow conditions of each of the phases inside the pipe change, the resulting frequencies will also change. On the other hand, given the signal strength at 2 different frequencies, it can be inferred that there is a large amount of energy associated with the passage of the bubble along the pipe, therefore, high intensity vibrations are caused that can end up generating structural failures if that situation is prolonged in time.

When those results are collected, analysis of fatigue must be made and, in this context, similar results such Fan et al. (2020) must be obtained, where were compared some situations of heating (or cooling) with and without random vibrations applied in elements called TSV-Cu, which installed in microelectronic devices of type PCB (printed circuit board).

In the case of this work, analysis of fatigue must be done in the sense to relate the cycle of fatigue of life for particular situation of two-phase flow and to transform these results in operation time. For example, consider the result obtained by Fan et al. (2020) as indicate below:

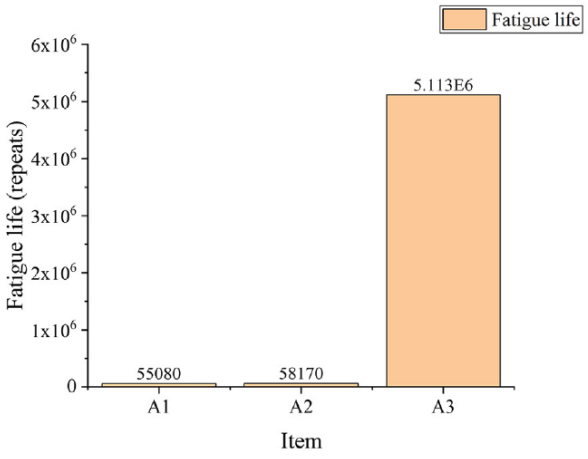

(d) Fatigue life

Figure 3.2. Fatigue in life for different situations analyzed.
Source: Fan et al. (2020).

We are going to suppose that for this work, A1, A2 and A3 represent three different flow conditions: A1 is a slug pattern flow; A2 is a churn pattern flow; and, A3 is a bubble pattern flow. According to Figure 3.2, the intermittence of the two-phase flow causes a shorter life of the structure (i.e., in the safety valve). Thus, for the information to have an even more practical reading, the term "*cycles* or *repeats*" must be changed. For example, let us define: ***1 cycle*** = $L_{liquid\_piston} + L_{Taylor\_bubble}$. Then, with this information it is possible to mention that the valve will fail for "X" liquid piston and Taylor bubble length. Consequently, using a high velocity camera in the laboratory, the velocity of the two-phase flow is determined for each experimental situation plotted on the flow map (see Figure 2.6) and, finally, the length (or cycle) and velocity are transformed into time, which can be measured in unit of year, for example. In this way, maintenance times can be properly programmed to avoid failure of the safety valve, in case it is needed in a specific situation.

It is important to mention that, to determine the fatigue life of the structure (safety valve), a mathematical expression presented by Fan et al. (2020) should be used. In this context, the total strain amplitude (ε_a) is calculated as:

$$\varepsilon_a = \varepsilon_{ea} + \varepsilon_{pa} = \frac{\sigma_f'}{E}(2N)^b + \varepsilon_f'(2N)^c \tag{3}$$

Where ε_{ea} is the elastic deformation amplitude, ε_{pa} is the plastic deformation amplitude, σ'_f is the fatigue strength coefficient, N is the number of cycles, ε'_f is the fatigue ductility coefficient and, b and c are the fatigue strength exponent and fatigue ductility exponent, respectively.

Note in the Equation 3, the elastic and plastic deformation are considered simultaneously. Therefore, it is important to know the fatigue curve of the material for the analysis, as can be seen in the following figure (see Figure 3.3).

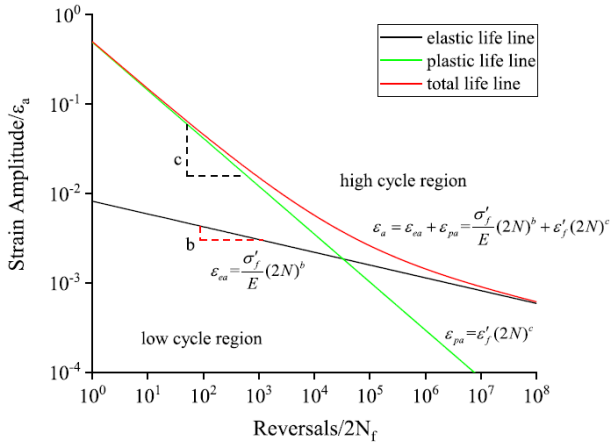

Figure 3.3. Fatigue curve of cupper employed in the work by Fan et al. (2020).

4. CONCLUSIONS

In this work was presented an analysis that will allow to determine in a practical way, the relationship between a two-phase flow and the mechanical vibrations produced in a safety valve (DHSV) installed in offshore oil wells. For this purpose, efforts will focus on devising an experimental bench on a small scale, which will allow experiments to be carried out at the LEMI at the University of Sao Paulo, Brazil. In this context, studies of structural and flow similarity were considered, but posteriorly, the extrapolation of the real-scale results must be done to analyze a real situation and determine if there is effectively a relationship between valve failures and flow conditions.

5. ACKNOWLEDGEMENTS

This work is being supported by Petrobras and FAFq (from Portuguese, *Fundação de Apoio à Física e à Química*) of Brazil.

6. REFERENCES

Cabrera-Miranda, J.M.; Paik, J.K. 2019. Two-Phase Induced Vibrations in a Marine Riser Conveying a Fluid with Rectangular Pulse Train Mass. *Ocean Engineering* 174: 71-83.

Carvalho, F.; Figueiredo, M.; Serpa, A. 2020. Flow Pattern Classification in Liquid-Gas Flows Using Flow-Induced Vibration. *Experimental Thermal and Fluid Science* 112: 109950.

Çengel, Y.A.; Cimbala, J.M. 2006. *Mecánica de Fluidos. Fundamentos y Aplicaciones*. Mc Graw Hill, 961 pp.

Fan, Z.; Liu, Y.; Chen, X.; Jiang, Y.; Zhang, S.; Wang, Y. 2020. Research on Fatigue of TSV-Cu Under Thermal and Vibration Coupled Load Based on Numerical Analysis. *Microelectronic Reliability* 106: 113590.

Li, F.; An, C.; Duan, M.; Su, J. 2020. Combined Damping Model for Dynamics and Stability of a Pipe Conveying Two-Phase Flow. *Ocean Engineering* 195: 106683.

Matos, P.H.M.C.; Das Neves, D.A.; Vieira, S.C.; Der Geest, C.V.; Iceri, D.M.; Castro, M.S.; Fabro, A.T. 2022. Analytical and Experimental Investigation of Flexural Waves in Horizontal Pipes Conveying Two-Phase Periodic Intermittent Flow. *Applied Acoustic* 192: 108714.

Miwa, S.; Mori, M.; Hibiki, T. 2015. Two-Phase Flow Induced Vibration in Piping Systems. *Progress in Nuclear Energy* 78: 270-284.

Ni, P.; Li, J.; Hao, H.; Xia, Y.; Du, X. 2019. Stochastic Dynamic Analysis of Marine Risers Considering Fluid-Structure Interaction and System Uncertainties. *Engineering Structures* 198: 109507.

Norma API 14A, 2015. Specification for Subsurface Safety Valve Equipment. American Petroleum Institute (API), Washington DC, EUA.

Ortega, A.; Rivera, A.; Larsen, C.M. 2018. Slug Flow and Waves Induced Motions in Flexible Riser. *Journal of Offshore Mechanics and Arctic Engineering* 140(1): 011703-1-011703-9.

Païdoussis, M.P. 2014. *Fluid-Structure Interactions. Slender Structures and Axial Flow. Volume 1*. Elsevier Ltd., 867 pp.

Ribeiro, P. M. V.; Pedroso, L. J. 2016. Uma Abordagem com Superposição Modal para Problemas de Interação Fluido-Estrutura. *Revista Internacional de Métodos Numéricos para Cálculo y Diseño en Ingeniería* 32(2): 79-90.

Shoham, O. 2005. *Mechanic Modeling of Gas-Liquid Two-Phase Flow in Pipes*. The Society of Petroleum Engineers (SPE), 310pp.

Taitel, Y.; Bornea, D.; Dukler, A. E. 1980. Modelling Flow Pattern Transitions for Steady Upward Gas-Liquid Flow in Vertical Tubes. *AIChE Journal* 26(3): 345-354.

Tian, Z.; Liu, F.; Zhou, L.; Yuan, C. 2020. Fluid-Structure Interaction Analysis of Offshore Structures Based on Separation of Transferred Responses. *Ocean Engineering* 195: 106598.

Wang, L.; Yang, Y.; Li, Y.; Wang, Y. 2018. Dynamic Behaviors of Horizontal Gas-Liquid Pipes Subjected to Hydrodynamic Slug Flow: Modelling and Experiments. *International Journal of Pressure Vessels and Piping* 161: 50-57.

Zhu, H.; Gao, Y.; Zhao, H. 2019. Experimental Investigation of Slug Flow-Induced Vibration of a Flexible Riser. Ocean Engineering, 189, 106370.

7. RESPONSIBILITY NOTICE

The authors are the only responsible for the printed material included in this paper.